Fundamentals of Analog VLSI Design
Exercise 12 - Solution

Design of Continuous-time Filters

Christian Enz (christian.enz@epfl.ch)

10.12.2025

1 Problem 1: Design of a cascade G_m-C continuous-time filter

1.1 Filter specifications

We want to design a low-pass filter that satisfies the specifications given in Table 1.1 using a Butterworth approximation.

Table 1.1: Filter specifications.

Specification	Symbol	Value	Unit
Cut-off frequency	f_c	20	kHz
Stop-band frequency	f_s	120	kHz
Pass-band gain	G_p	-1	dB
Stop-band gain	G_s	-40	dB

The filter mask corresponding to the specifications of Table 1.1 is shown in Figure 1.1.

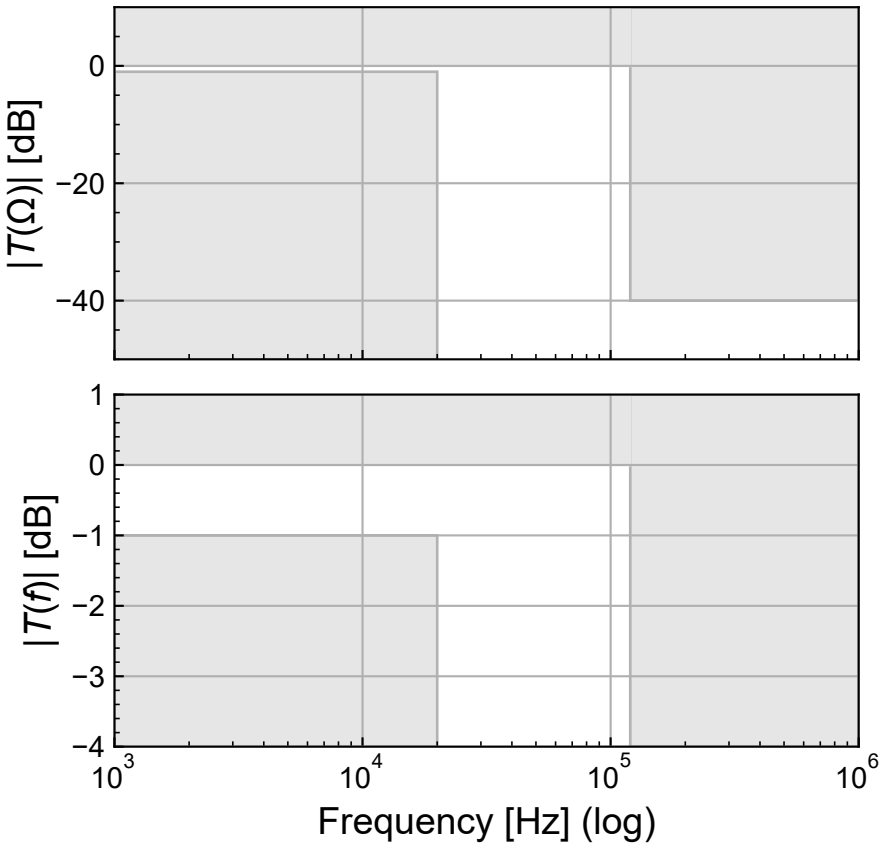

Figure 1.1: Filter mask.

We now recall the basics of the Butterworth approximation that will then be reused for the design.

1.2 Butterworth approximation

If we choose a Butterworth approximation, we first calculate the parameter ε related to the maximum attenuation A_p in the passsband and given by

$$\varepsilon = \sqrt{10^{\frac{A_p}{10}} - 1} \tag{1.1}$$

where $A_p = -G_p$ is the attenuation in the pass-band. The minimum order is then estimated according to

$$N_{est} = \frac{\log\left(\frac{10^{A_s/10}-1}{10^{A_p/10}-1}\right)}{2\log(\Omega_s)}, \tag{1.2}$$

where $A_s = -G_s$ is the attenuation in the stop-band and $\Omega_s \triangleq f_s/f_p$. The order is then the integer immediately larger than N_{est}.

It can be shown that the poles p_k of the Butterworth function are all located on a circle of radius

$$\omega_0 = \varepsilon^{-\frac{1}{N}} \cdot \omega_p \tag{1.3}$$

and are given by

$$p_k = \omega_0 e^{j\left(\frac{\pi}{2}+\frac{2k-1}{2N}\pi\right)} = \omega_0\left[\cos\left(\frac{2k+N-1}{2N}\pi\right) + j\sin\left(\frac{2k+N-1}{2N}\pi\right)\right]. \tag{1.4}$$

for $k = 1, 2, \cdots, N$. There are $N/2$ complex conjugated poles and for N odd there is an additional real pole located at $-\omega_0$.

A transfer function having a pair of complex conjugated poles given by

$$p_{1,2} = \sigma_p \pm j\omega_p \tag{1.5}$$

can be written as

$$T(s) = \frac{N(s)}{s^2 + \frac{\omega_0}{Q}s + \omega_0^2}, \tag{1.6}$$

where the poles can be expressed as

$$p_{1,2} = -\frac{\omega_0}{2Q} \pm j\omega_0\sqrt{1 - \frac{1}{(2Q)^2}}. \tag{1.7}$$

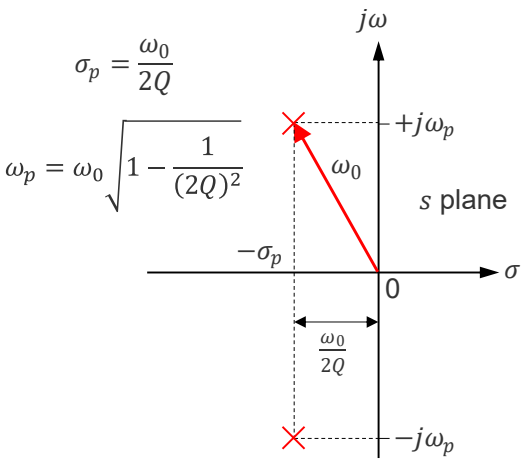

Figure 1.2: Butterworth low-pas filter transfer function magnitude.

The resonance frequency ω_0 and the quality factor Q are given by

$$\omega_0 = \sqrt{p_1 p_2}, \tag{1.8}$$

$$Q = \frac{\omega_0}{2\sigma_p} = -\frac{\omega_0}{p_1 + p_2} = -\frac{\sqrt{p_1 p_2}}{p_1 + p_2}. \tag{1.9}$$

They are related to the poles according to

$$p_1 p_2 = \sigma_p^2 + \omega_p^2 = \omega_0^2, \tag{1.10}$$

$$-(p_1 + p_2) = 2\sigma_p = \frac{\omega_0}{Q}. \tag{1.11}$$

The Butterworth transfer function can now be written as

$$T(s) = K \cdot \frac{\omega_0^N}{(s - p_1)(s - p_2)...(s - p_N)}, \tag{1.12}$$

where K sets the dc gain. Since for N even, the product of the N poles can be grouped into the product of $N/2$ pairs of complex conjugated poles each being equal to ω_0^2, resulting in $(\omega_0^2)^{N/2} = \omega_0^N$. For N odd, the product of the N poles can be grouped into the product of $(N-1)/2$ pairs of complex conjugated poles each being equal to ω_0^2 times the real pole equal to ω_0 resulting in $(\omega_0^2)^{(N-1)/2}\omega_0 = \omega_0^N$.

Pairing the complex conjugated poles leads to

$$T(s) = K \cdot \prod_{k=1}^{M} \frac{\omega_0^2}{s^2 + \frac{\omega_0}{Q_k} s + \omega_0^2} \times \begin{cases} 1 & \text{for } N \text{ even}, \\ \frac{\omega_0}{s+\omega_0} & \text{for } N \text{ odd}. \end{cases} \tag{1.13}$$

with $M = N/2$ for N even and $M = (N-1)/2$ for N odd.

The quality factors Q_k of each second-order section are given by

$$Q_k = \frac{1}{2\sin\left(\frac{2k-1}{2N}\pi\right)} \text{ for } k = 1, 2, \cdots, M. \tag{1.14}$$

This shows that for the Butterworth approximation, we only need to calculate the resonance frequency ω_0, which is common to all the second-order functions (and the eventual first-order for n odd), using (1.8) and the quality factors Q_k according to (1.14).

1.3 Order estimation and filter parameters calculation

For the specifications given in Table 1.1, we have $\varepsilon = 0.508847$, $\Omega_s = 6$ and $N_{est} = 2.947230$. This requires an order $N = 3$. The transfer function can then be written as

$$T(s) = \frac{\omega_0}{s + \omega_0} \cdot \frac{\omega_0^2}{s^2 + \frac{\omega_0}{Q} s + \omega_0^2}. \tag{1.15}$$

The resonance frequency is then derived from the normalized radius

$$\Omega_0 \triangleq \frac{\omega_0}{\omega_p} = \varepsilon^{-\frac{1}{N}}, \tag{1.16}$$

leading to $\Omega_0 = 1.252576$ and $\omega_0 = \Omega_0\, \omega_p = 2\pi\, f_0 = 2\pi\ 25.051528\ krad/s$. The quality factor Q is calculated using (1.14) resulting in $Q = 1$. The magnitude of the corresponding transfer function is plotted in Figure 1.3. We see that the chosen Butterworth approximation just fits within the filter mask, but there are no margins. Normally you would add some margins to account for the tolerance on the filter components.

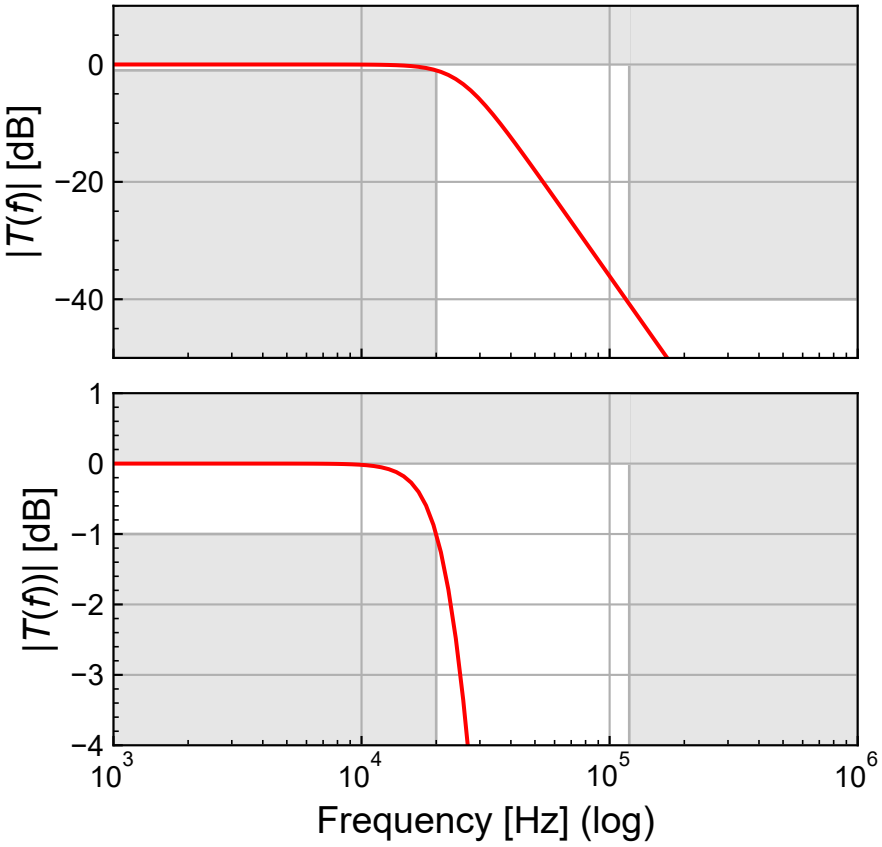

Figure 1.3: Filter transfer function.

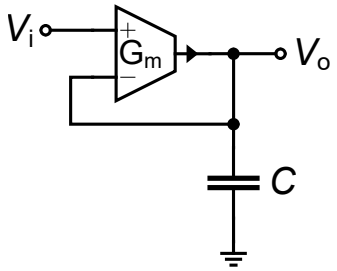

Figure 1.4: G_m-C 1st-order section.

1.4 G_m-C filter implementation

There are several solutions for implementing the desired transfer function with a G_m-C filter. Since the order is odd, we need a 1st-order section. We can choose the simplest 1st-order section shown in Figure 1.4 which transfer function is given by

$$T(s) = \frac{\omega_c}{s + \omega_c} \tag{1.17}$$

with $\omega_c = G_m/C$.

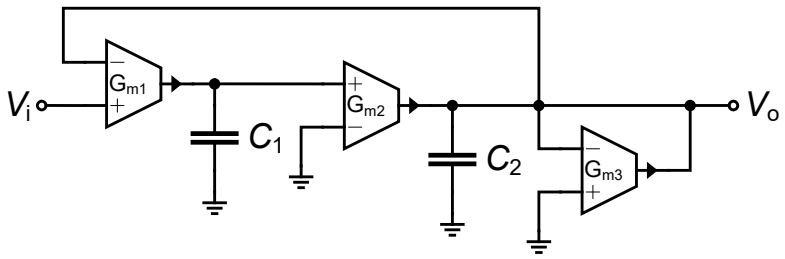

Figure 1.5: G_m-C 2nd-order section.

The 2nd-order section can be implemented by the Tow-Thomas 2nd-order section shown in Figure 1.5 which has the following transfer function

$$T(s) = \frac{\omega_0^2}{s^2 + \frac{\omega_0}{Q}\, s + \omega_0^2} \tag{1.18}$$

with

$$\omega_0 = \sqrt{\frac{G_{m1}}{C_1} \cdot \frac{G_{m2}}{C_2}}, \tag{1.19}$$

$$Q = \sqrt{\frac{C_2}{C_1}} \cdot \frac{\sqrt{G_{m1} \cdot G_{m2}}}{G_{m3}}. \tag{1.20}$$

In this design we can choose all the G_m to be equal $G_{m1} = G_{m2} = G_{m3} = G_m$ and because $Q = 1$ we can also choose all the capacitances to be equal $C_1 = C_2 = C$ resulting in

$$\omega_0 = \frac{G_m}{C}, \tag{1.21}$$

$$Q = 1. \tag{1.22}$$

This which leads to the final filter shown in Figure 1.6, where all the OTAs are identical and all the capacitances have the same value.

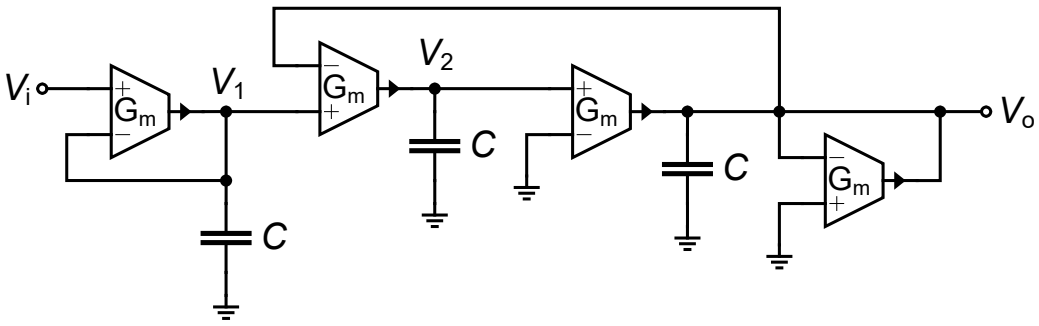

Figure 1.6: Complete 3rd-order low-pass G_m-C filter.

The transconductance G_m or capacitance C still need to be set for the given specifications. We can use an additional constraint on the total integrated thermal noise at the output. If we assume that all the OTAs contribute equally to the output noise, which is not exactly correct, but is a good first-order estimation, then

$$V_{nout}^2 \cong 4 \cdot \frac{\gamma_n \, k \, T}{C}, \tag{1.23}$$

where we assumed that all OTAs have the same thermal noise excess factor γ_n. We can now estimate the smallest value of the capacitance to meet the integrated noise specification as

$$C_{min} \cong 4 \cdot \frac{\gamma_n \, k \, T}{V_{nout}^2} \tag{1.24}$$

For $V_{nout} = 120 \ \mu V_{rms}$ with $\gamma_n = 2$, we get $C_{min} = 2.301 \ pF$. Choosing $C = 2.4 \ pF$ gives $V_{nout} = 118 \ \mu V_{rms}$. The transconductance follows as $G_m = 378 \ nA/V$.

We can now check the resulting transfer function by simulations using an ideal model for the OTAs (basically a VCCS).

1.5 Simulations

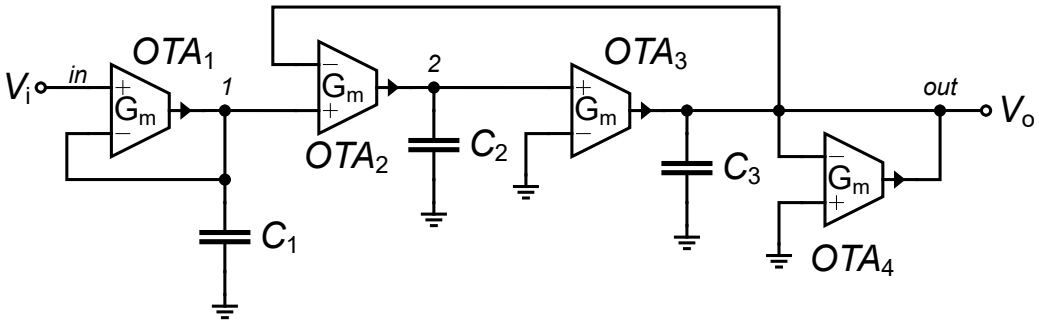

Figure 1.7: 3rd-order low-pass G_m-C filter schematic used for simulations.

We can now check the transfer function using ngspice with the circuit schematic shown in Figure 1.7. The OTAs are considered as ideal VCCS to which we add a noise current with PSD $\gamma_n \, G_m$. They are implemented as a subcircuit described below:

```
* Ideal single-ended OTA
.subckt OTA in+ in- out Gmval=1e-6 gammanval=2
Rn 1 0 {gammanval/Gmval}
G1 0 out in+ in- {Gmval}
Gn 0 out 1 0 {Gmval}
Go out 0 out 0 1e-15
.ends Gm
```

> **Note**
>
> Note that the VCCS Go is simulating a noiseless output resistance that sets the DC gain.

The simulated transfer function is compared to the theoretical transfer function in Figure 1.8. We see a perfect agreement.

Figure 1.9 shows the simulated contributions of individual OTAs to the output white noise PSD together with the total output white noise PSD.

We see in Figure 1.9 that the output noise PSD in the passband is dominated by OTA_1, OTA_2 and OTA_3, whereas above the cut-off frequency the output noise PSD is dominated by OTA_4.

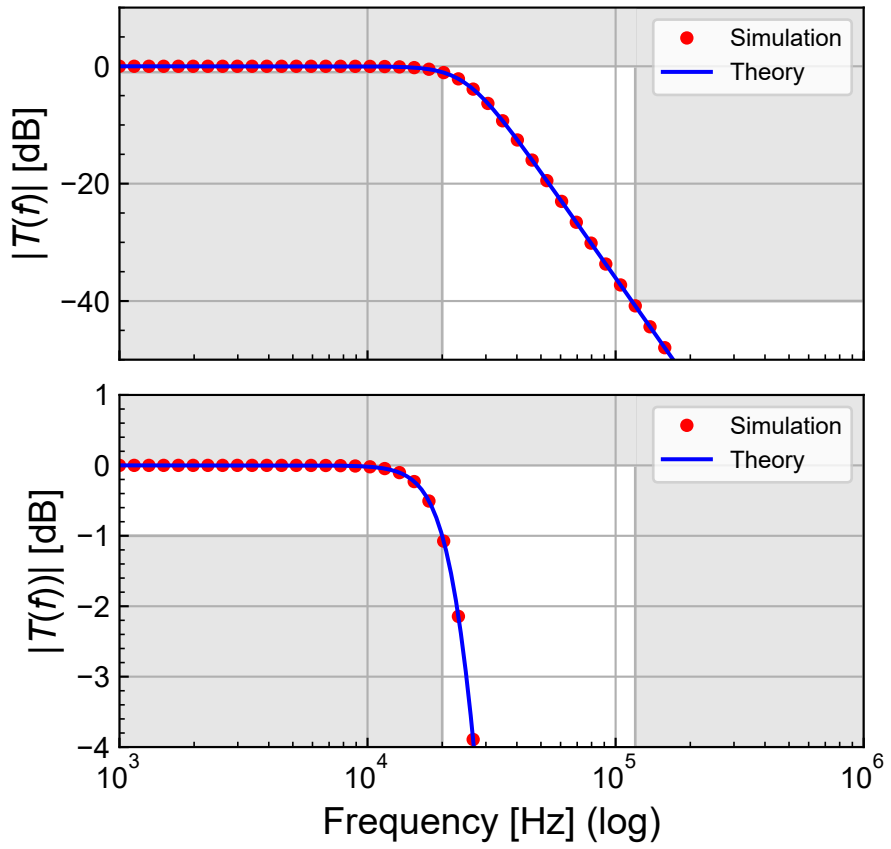

Figure 1.8: Simulated transfer function.

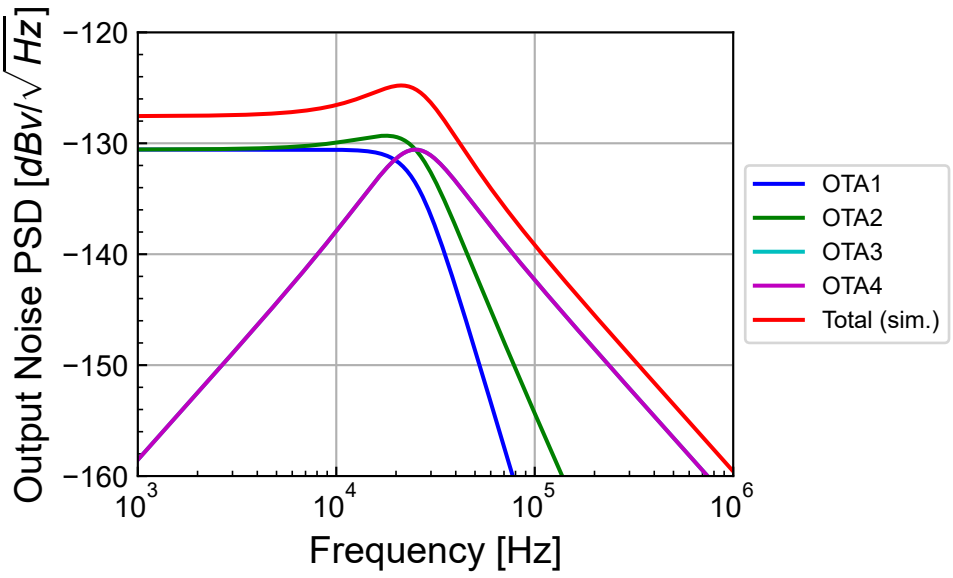

Figure 1.9: Simulated output-referred noise PSD.

In ngspice we can also extract the integrated noise. The contributions of individual OTAs to the output integrated white noise are presented in Table 1.2 together with the total output integrated white noise. We see that it is slightly lower than the value estimated initially $V_{nout} = 118\ \mu V_{rms}$. A detailed analysis shows that the total output integrated white noise power, assuming all OTAs have the same thermal noise excess factor γ_n, is actually given by

$$V_{nout}^2 = \frac{11}{3}\frac{\gamma_n\, kT}{C}, \tag{1.25}$$

which is close to the original assumption $V_{nout}^2 \cong 4\,\gamma_n\, kT/C$. The value estimated from (1.25) is given in Table 1.2. We see that it is close to the simulated value. The difference comes from the integration range which is smaller for the simulation than the theoretical bounds.

Table 1.2: Integrated output noise voltages.

OTA	Symbol	Value	Unit
OTA1	V_{nout1}	47	μV_{rms}
OTA2	V_{nout2}	58	μV_{rms}
OTA3	V_{nout3}	58	μV_{rms}
OTA4	V_{nout4}	58	μV_{rms}
Total (simulation)	V_{nout}	111	μV_{rms}
Total (theory)	V_{nout}	112	μV_{rms}

The next step would be to replace the ideal OTAs with OTAs realized with transistors.

2 Problem 2: Design of a G_m-C continuous-time filter using the LC ladder approach

2.1 The LC ladder approach

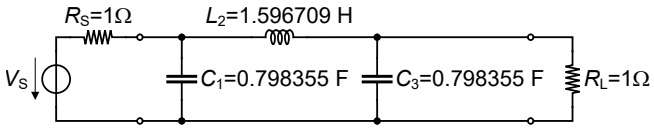

Figure 2.1: Low-pass prototype filer (LPPF) for a Butterworth approximation.

In this problem, we want to design a G_m-C filter that satisfies the same specifications given in Table 1.1 and used for Problem 1 and the same filter mask shown in Figure 1.1. We also will use a Butterworth approximation with the transfer function shown in Figure 1.3. The difference is that for this G_m-C implementation, we propose to use the indirect simulation of an LC ladder approach. To this purpose we start from the low-pass prototype filter (LPPF) shown in Figure 2.1 which implements a Butterworth approximation with $\Omega_s = \omega_s/\omega_p = 6$. The normalized components values for a Butterworth approximation are given in Table 2.1. The normalized transfer function corresponding to the LPPF is shown in Figure 2.2.

Table 2.1: Values of the LPPF components for a Butterworth approximation.

Symbol	Value	Unit
C_1	0.798355	F
L_2	1.59671	H
C_3	0.798355	F

In the direct simulation approach we start writing the state equations of the LC-ladder filter shown in Figure 2.3. The current and voltage equations of the LC ladder filter shown in Figure 2.3 are given by

$$I_1 = \frac{V_{in} - V_2}{R_1}, \tag{2.1}$$

$$V_2 = \frac{I_1 - I_3}{sC_2}, \tag{2.2}$$

$$I_3 = \frac{V_2 - V_4}{sL_3}, \tag{2.3}$$

$$V_4 = V_{out} = \frac{I_3 - I_5}{sC_4}, \tag{2.4}$$

$$I_5 = \frac{V_4}{R_5}. \tag{2.5}$$

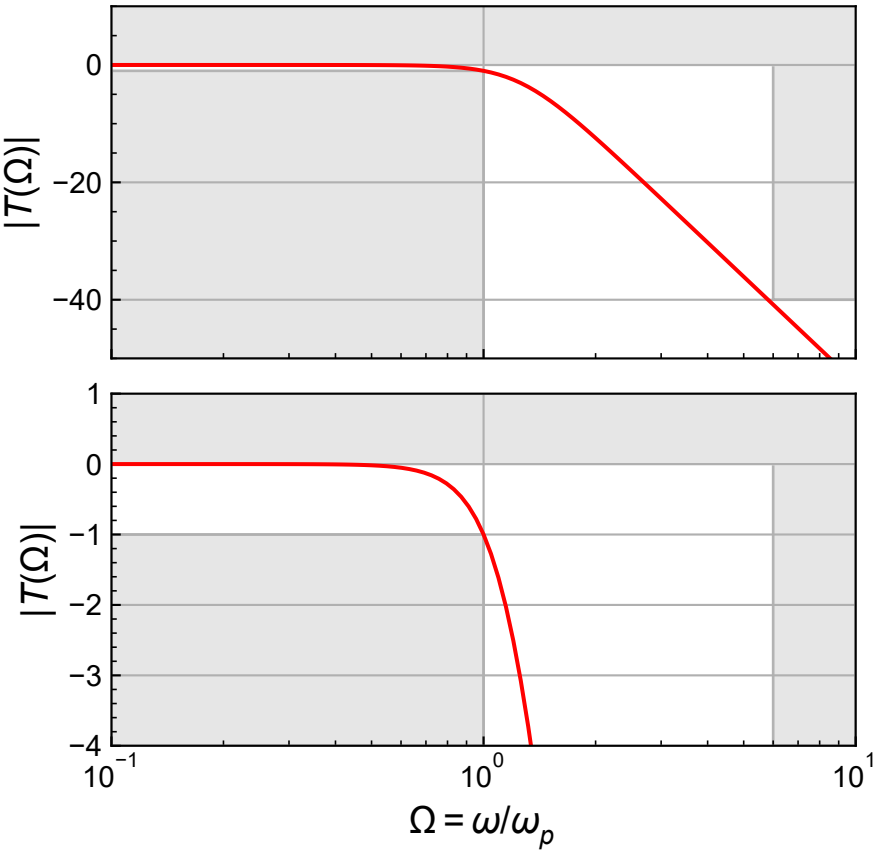

Figure 2.2: Normalized transfer function.

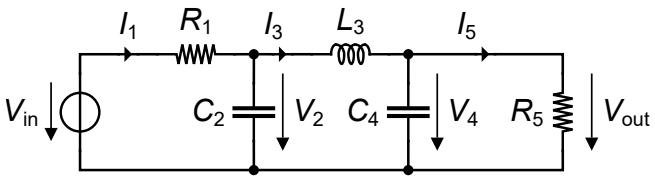

Figure 2.3: 3rd-order LC low-pass filter.

Multiplying the currents by a normalization impedance Z_0 leads to

$$V_1 \triangleq Z_0 \cdot I_1 = \frac{Z_0}{R_1} \cdot (V_{in} - V_2), \tag{2.6}$$

$$V_2 = \frac{V_1 - V_3}{sZ_0C_2}, \tag{2.7}$$

$$V_3 \triangleq Z_0 \cdot I_3 = \frac{Z_0}{sL_3} \cdot (V_2 - V_4), \tag{2.8}$$

$$V_4 = V_{out} = \frac{V_3 - V_5}{sZ_0C_4}, \tag{2.9}$$

$$V_5 \triangleq Z_0 \cdot I_5 = \frac{Z_0}{R_5} \cdot V_4. \tag{2.10}$$

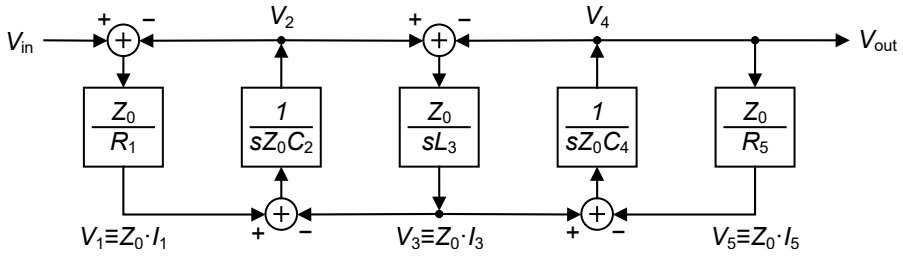

Figure 2.4: Signal-flow diagram corresponding to the LC ladder of Figure 2.3.

The above equations can be represented by the signal flow graph (SFG) shown in Figure 2.4. We can set $Z_0 = R_5$ which simplifies the SFG of Figure 2.4 to the one shown in Figure 2.5.

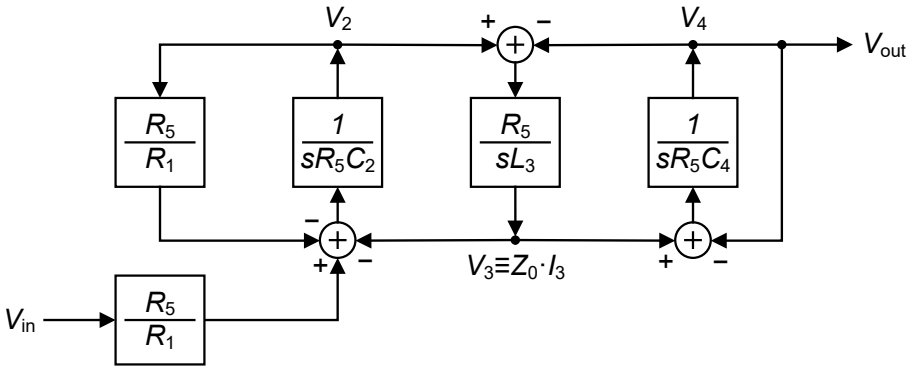

Figure 2.5: Simplification the SFG of Figure 2.4 after setting $Z_0 = R_5$.

In order to compensate for the unavoidable loss observed in the passband of the passive LC implementation, the input has been added separately to the summation at the input of the first integrator. This will allow to compensate for the loss without modifiying the filter characteristic as shown in Figure 2.6.

As shown in Figure 2.6, all the branches can be implemented by summing integrators except the first and last branches resulting in the SFG shown in Figure 2.7 where the integrator time constants are given by

$$\tau_1 \triangleq R_5C_2, \tag{2.11}$$

$$\tau_2 \triangleq \frac{L_3}{R_5}, \tag{2.12}$$

$$\tau_3 \triangleq R_5C_3. \tag{2.13}$$

The above time constants can be obtained by denormalizing the time constants of the LPPF according

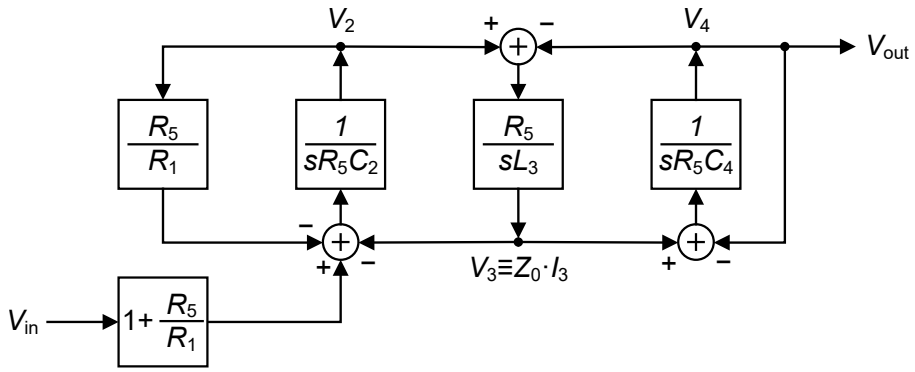

Figure 2.6: SFG of the 3rd-order LC low-pass filter adding the input separetly to correct for the loss in the passband.

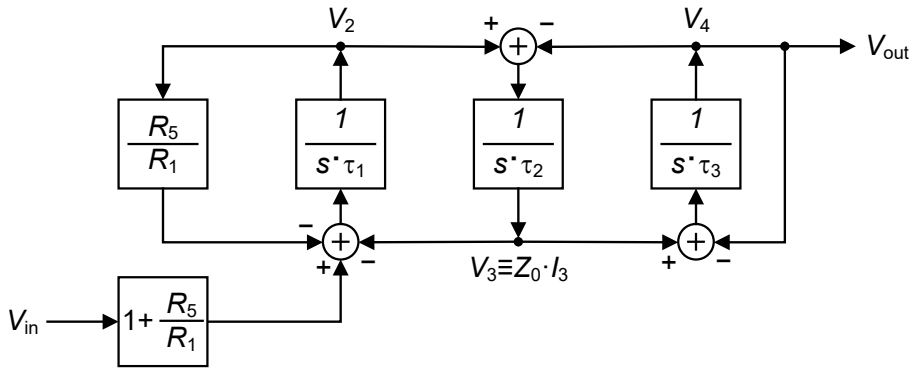

Figure 2.7: SFG of the 3rd-order LC low-pass filter with correction of the loss in the passband and showing the 3 integrators with their integration time constants.

to

$$\tau_1 = \frac{R_{norm}\, C_{1,norm}}{\omega_p}, \tag{2.14}$$

$$\tau_2 = \frac{L_{2,norm}}{R_{norm}\, \omega_p}, \tag{2.15}$$

$$\tau_3 = \frac{R_{norm}\, C_{3,norm}}{\omega_p}, \tag{2.16}$$

with $R_{norm} = R_S = R_L = 1\,\Omega$. The denormalized time constants are given in Table 2.2. We see that $\tau_1 = \tau_3 = \tau$ and $\tau_2 = 2\,\tau$.

Table 2.2: Denormalized time constants.

Symbol	Value	Unit
τ_1	6.35311	μs
τ_2	12.7062	μs
τ_3	6.35311	μs

2.2 Filter implementation with G_m-C integrators

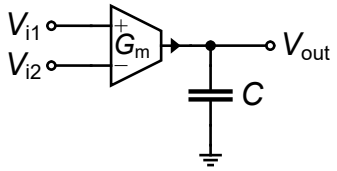

Figure 2.8: G_m-C integrator.

The SFG of Figure 2.7 can be implemented using the differential G_m-C integrator shown in Figure 2.8 and having the following transfer function

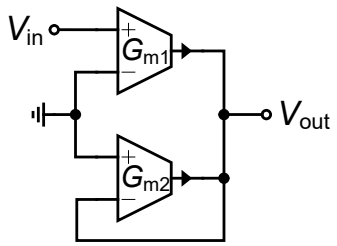

Figure 2.9: G_m-C gain stage.

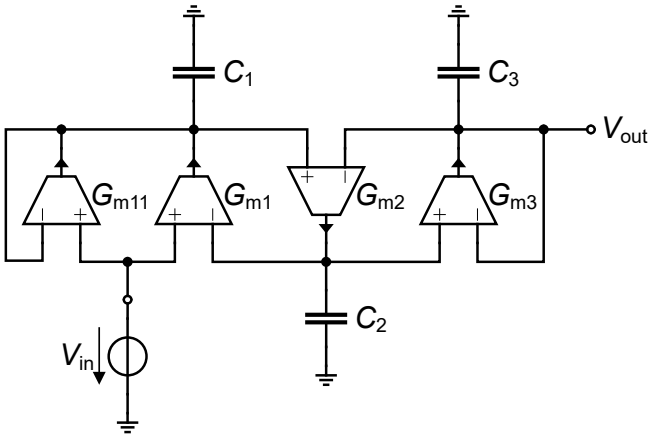

Figure 2.10: G_m-C filter implementation.

where we assume that OTA_1 and OTA_3 have the same thermal noise excess factor γ_n. We can then estimate the smallest value of the capacitance C as

$$C_{min} \cong 2\,\frac{\gamma_n\,kT}{V_{nout}^2}. \tag{2.20}$$

For $V_{nout} = 120\ \mu V_{rms}$ and $\gamma_n = 2$, we get $C_{min} = 1.151\ pF$. We finally choose $C_1 = 1.2\ pF$ which gives $V_{nout} = 118\ \mu V_{rms}$. The filter component values are given in Table 2.3.

Table 2.3: Component values of the G_m-C filter of Figure 2.10.

Symbol	Value	Unit
C_1	1.2	pF
C_2	2.4	pF
C_3	1.2	pF
G_m	188.884	nA/V

We can now verify the design by simulations.

2.3 Simulations

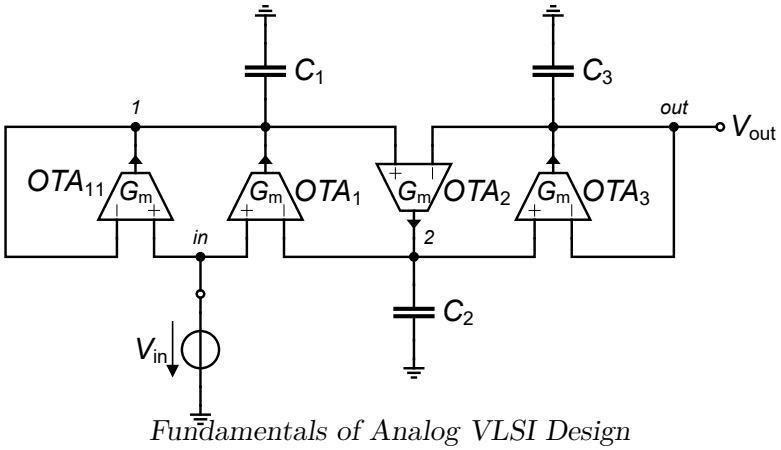

Figure 2.11: 3rd-order low-pass G_m-C filter schematic used for simulations

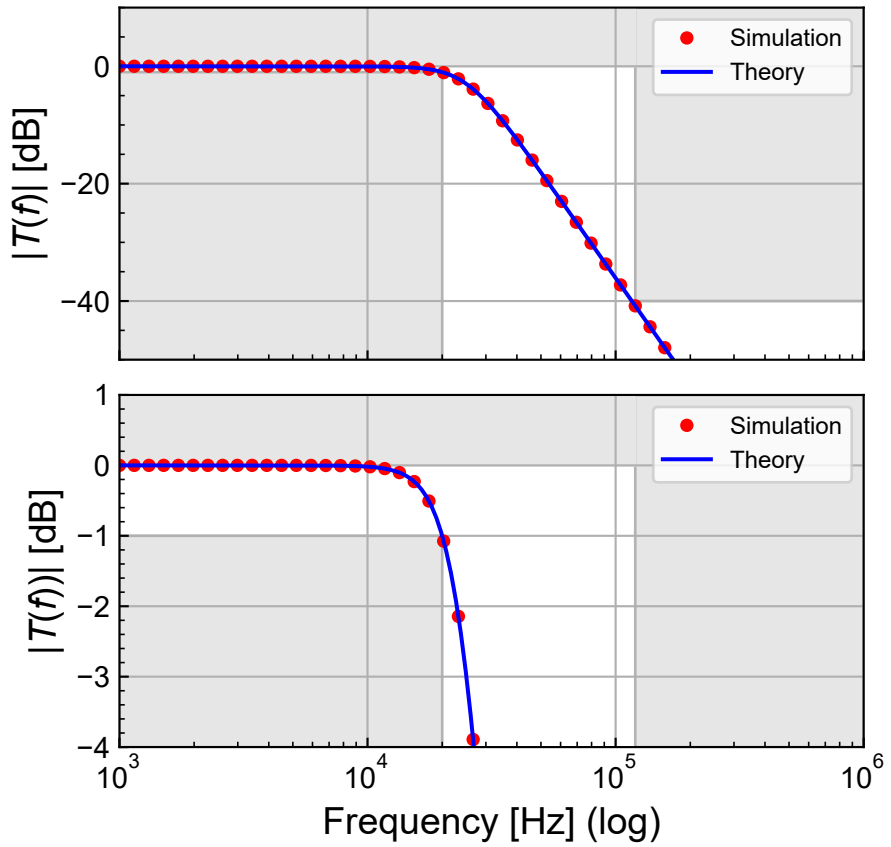

Figure 2.12: Simulated transfer function.

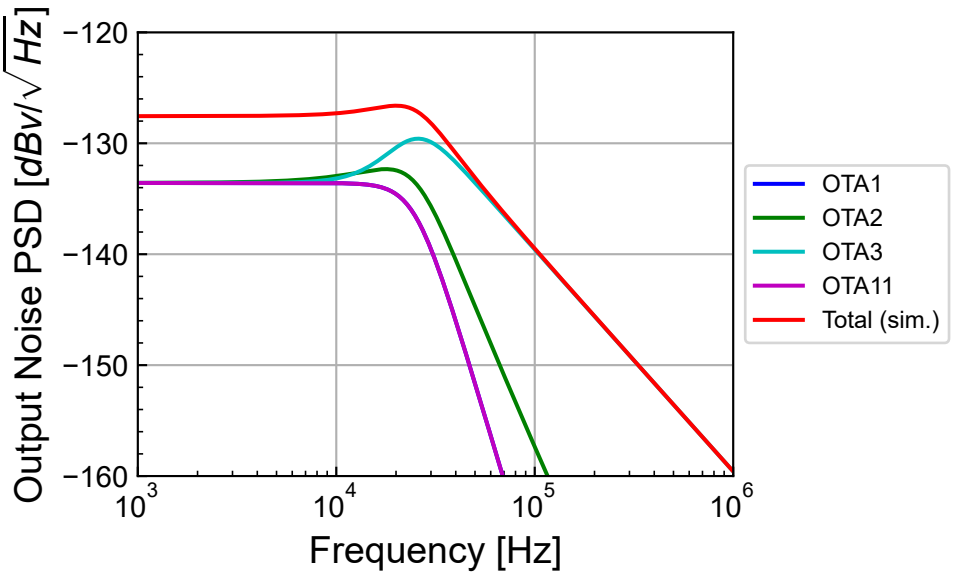

Figure 2.13: Simulated output-referred noise PSD.

which for the chosen capacitance $C = 1.2\ pF$ we get $V_{nout} = 99\ \mu V_{rms}$.

In ngspice we can also extract the integrated noise. The contributions of individual OTAs to the output integrated white noise are presented in Table 2.4 together with the total output integrated white noise. We see that the simulated integrated output noise voltage is very close to the theoretical estimation.

Table 2.4: Integrated output noise voltages.

OTA	Symbol	Value	Unit
OTA1	V_{nout1}	33	μV_{rms}
OTA2	V_{nout2}	41	μV_{rms}
OTA3	V_{nout3}	75	μV_{rms}
OTA11	V_{nout11}	33	μV_{rms}
Total (sim)	V_{nout}	97	μV_{rms}
Total (theory)	V_{nout}	99	μV_{rms}

The next step would be to replace the ideal OTAs with OTAs realized with transistors.

3 Problem 3: Design of a MOSFET-C continuous-time filter

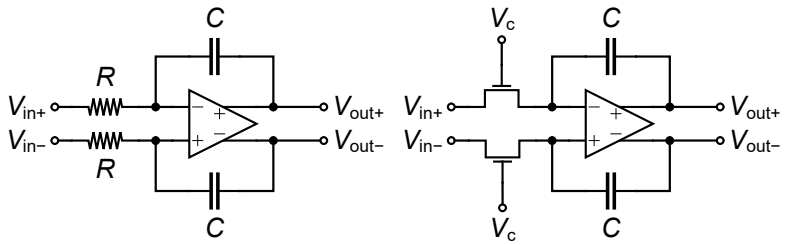

Figure 3.1: Fully-differential active-RC and MOSFET-C integrator.

We can also implement the filter corresponding to the SFG of Figure 2.7 with the fully-differential active-RC or MOSFET-C integrators shown in Figure 3.1 which have a transfer function given by

$$T(s) \triangleq \frac{V_{out}}{V_{in}} = -\frac{1}{s\,\tau} \tag{3.1}$$

with $\tau = RC$. The filter implemented with fully-differential active-RC integrators is shown in Figure 3.2.

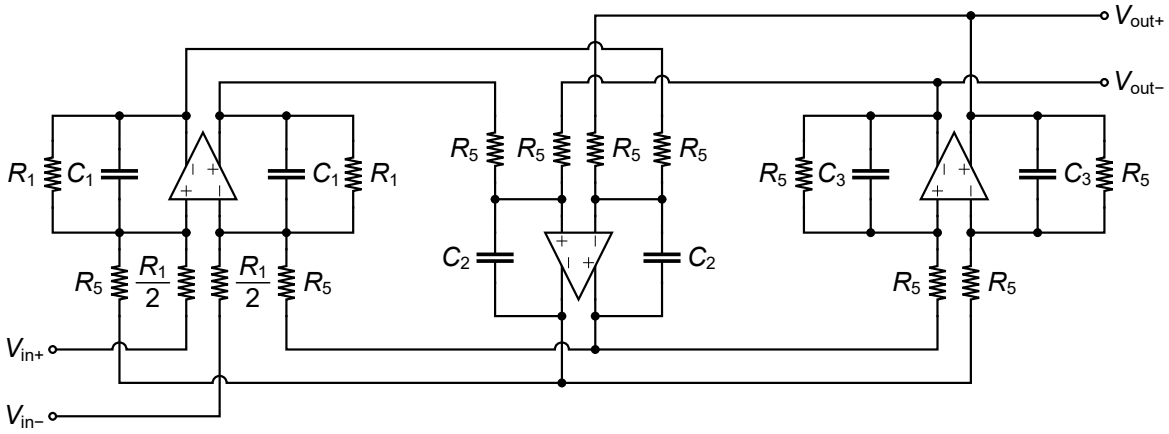

Figure 3.2: MOSFET-C implementation of the 3rd-order LP filter.

Notice the input resistance have values equal to $R_1/2$ in order to compensate for the $-6\,dB$ gain of the passive LC ladder filter.

For the particular Butterworth approximation, the source and load resistances are equal $R_1 = R_5 = R$. The latter can be set with an additional constraint for example on the total integrated thermal noise, which sets the minimum value of the capacitance.

If we assume that that the contribution of the OPAMP can be neglected and that the noise of each integrator is dominated by the contributions of the resistances, then the integrated thermal noise of the lossy integrator can simply be estimated as kT/C because the resistances impose at the same time the white noise level and the cut-off frequency. The total integrated thermal noise at the filter output can then be estimated as 3 times the contribution of a single integrator

$$V_{nout}^2 \cong 3 \cdot \frac{k\,T}{C}. \tag{3.2}$$

from which we can estimate the smallest value of the capacitance

$$C_{min} \cong 3 \cdot \frac{k\,T}{V_{nout}^2}, \tag{3.3}$$

For $V_{nout} = 120\ \mu V_{rms}$, we get $C_{min} = 0.863\ pF$. We finally choose $C_1 = 0.9\ pF$ which gives $R_5 = 7.059\ M\Omega$. The filter component values are given in Table 3.1.

Table 3.1: Values of the MOSFET-C filter components.

Symbol	Value	Unit
C_1	0.9	pF
C_2	1.8	pF
C_3	0.9	pF
R_1	7.059	$M\Omega$
R_5	7.059	$M\Omega$

We can now verify the design by simulations.

3.1 Simulation

The above design can be verified by simulations using either ngspice or LTSpice with the schematic shown in Figure 3.3 (drawn in LTSpice).

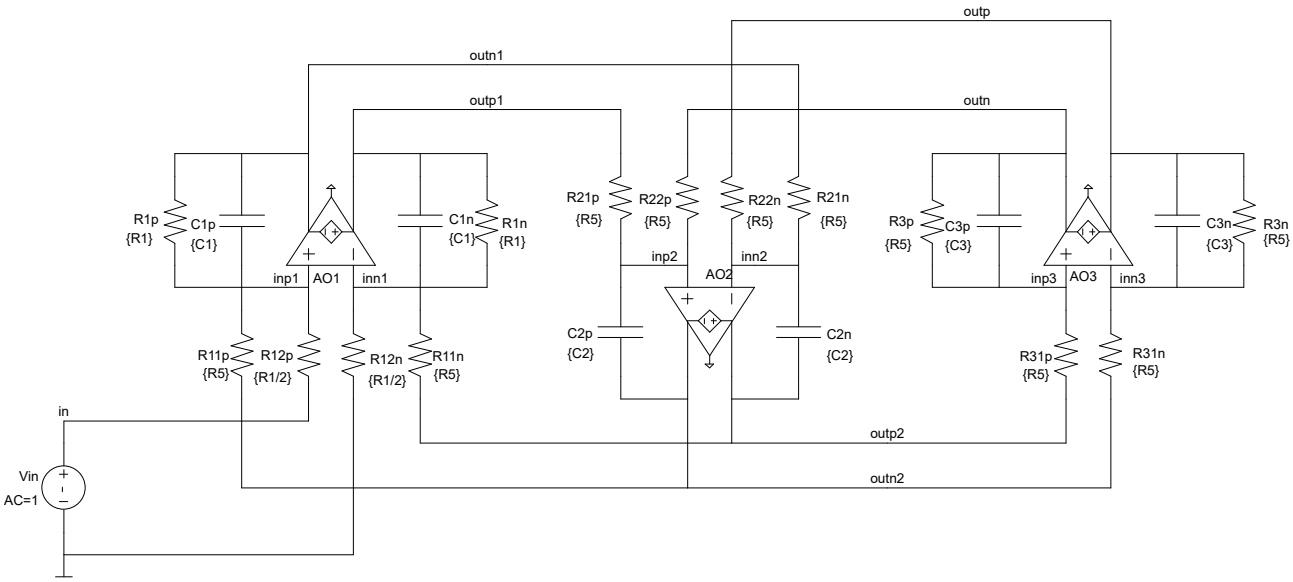

Figure 3.3: Schematic used for the ngspice simulation.

We will first simulate the filter with ngspice assuming ideal OPAMPs.

3.1.1 Ideal OPAMP

The simulated transfer function assuming ideal OPAMPs is compared to the theoretical transfer function in Figure 3.4. We see a perfect match between simulations and theory.

We now will investigate the effect of the OPAMP non-idealities such as a finite DC gain and a limited gain-bandwidth product.

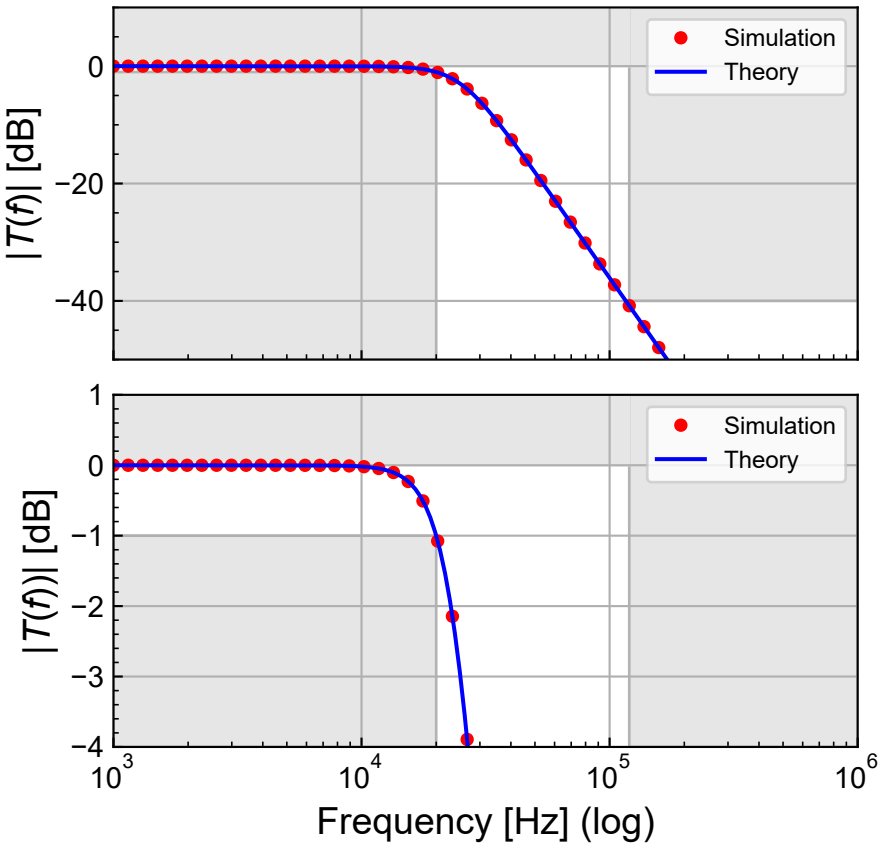

Figure 3.4: Simulated transfer function.

3.2 Non-ideal OPAMP

We can replace the ideal OPAMP with a subcircuit that accounts for the finite gain and finite bandwidth. Let's first investigate the effect of finite DC gain by setting the OPAMP DC gain to $A_{dc} = 40\ dB$ and the gain-bandwidth product to $GBW = 20\ MHz$. The open-loop gain of the nonideal OPAMP is shown in Figure 3.5. We see that the OPAMP has the desired frequency response. Let's now simulate the filter with this nonideal OPAMP.

From Figure 3.6 see that the OPAMP finite gain introduces some losses in the passband and the desired gain of 0 dB is no more reached. The resulting frequency response does not fit within the filter mask in the passband.

Let's now have a look at the effect of the finite bandwidth by setting the gain-bandwith product to 10 times the cut-off frequency $GBW = 200\ kHz$ and keeping a high OPAMP DC gain set to $A_{dc} = 100\ dB$. This results in the OPAMP open-loop gain response shown in Figure 3.7.

From Figure 3.8, we see that the limited gain-bandwidth product introduces some additional losses above the cut-off frequency and some undesired overshoot just before the cut-off frequency. The resulting frequency response does not fit within the filter mask in the passband because of this overshoot.

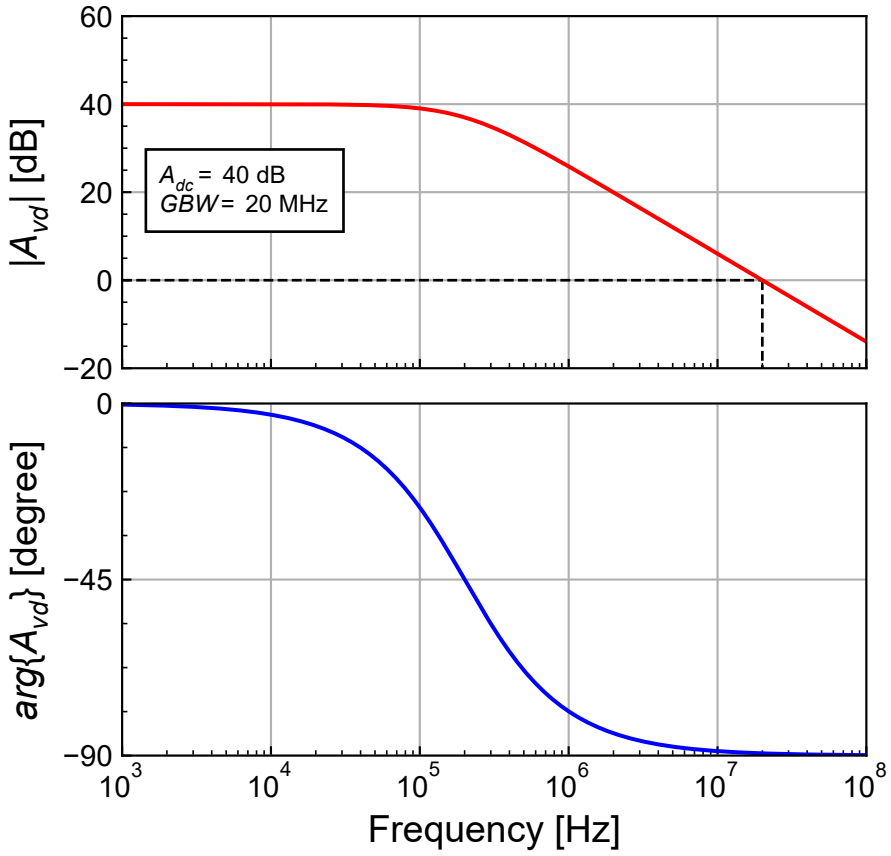

Figure 3.5: Open-loop gain of the non-ideal OPAMP with a low DC gain.

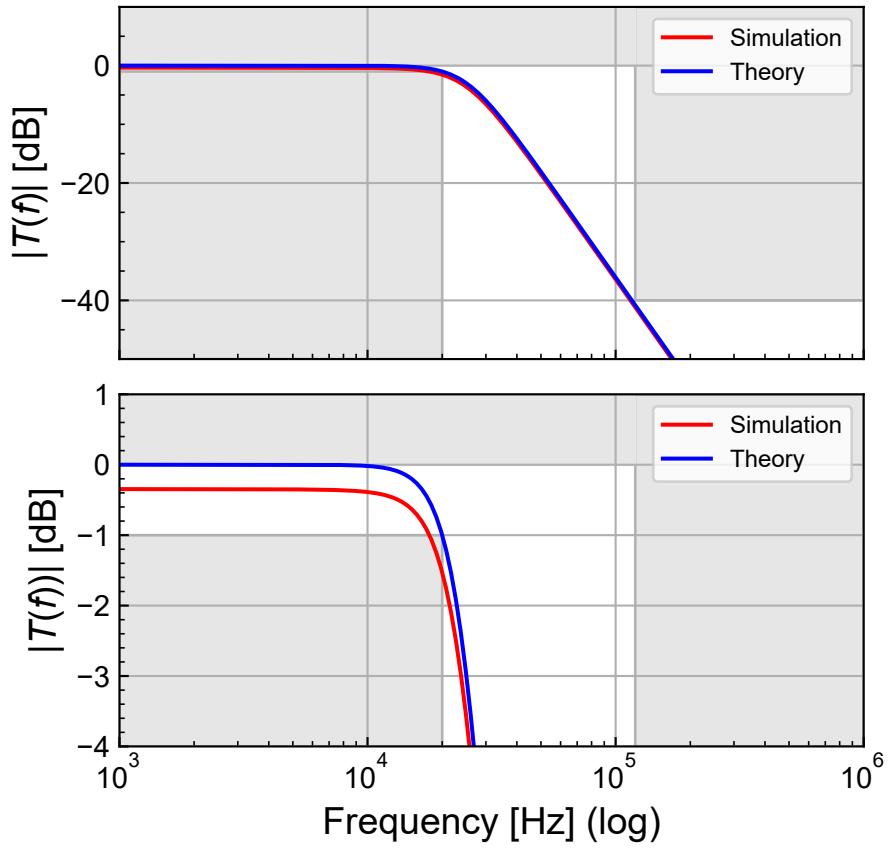

Figure 3.6: Simulated MOSFET-C filter transfer function including the effect of nonideal OPAMPs with low DC gain.

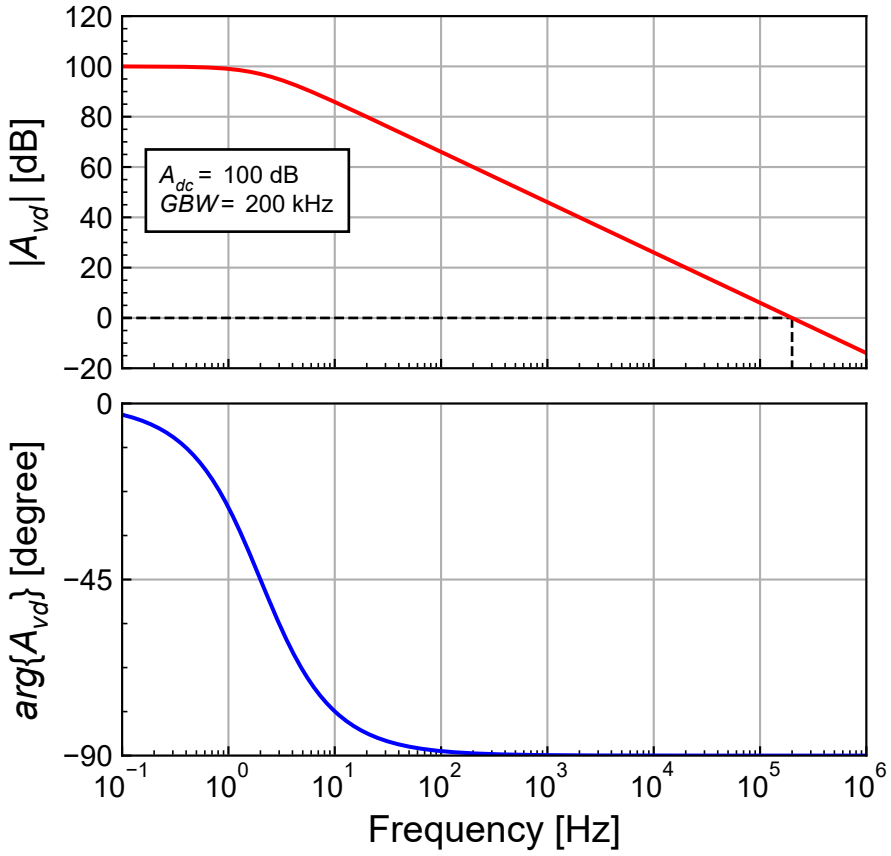

Figure 3.7: Open-loop gain of the non-ideal OPAMP with a low gain-bandwidth product.

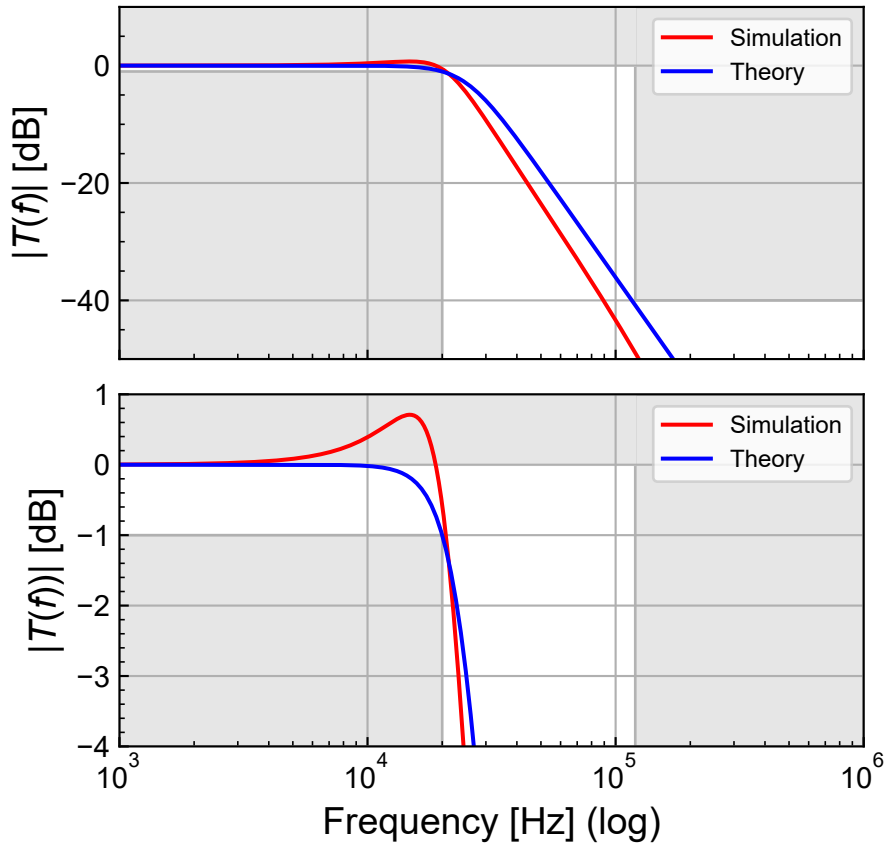

Figure 3.8: Simulated MOSFET-C filter transfer function including the effect of nonideal OPAMPs with low gain-bandwidth product.